Laser-induced breakdown spectroscopy of uranium in the vacuum ultraviolet range

E. Rollin, Olivier Musset, D. Cardona, J.-B. Sirven

▶ **To cite this version:**

E. Rollin, Olivier Musset, D. Cardona, J.-B. Sirven. Laser-induced breakdown spectroscopy of uranium in the vacuum ultraviolet range. Spectrochimica Acta Part B: Atomic Spectroscopy, 2020, 166, pp.105796. ⟨10.1016/j.sab.2020.105796⟩. ⟨hal-03489826⟩

HAL Id: hal-03489826

https://hal.science/hal-03489826v1

Submitted on 22 Aug 2022

HAL is a multi-disciplinary open access archive for the deposit and dissemination of scientific research documents, whether they are published or not. The documents may come from teaching and research institutions in France or abroad, or from public or private research centers.

L'archive ouverte pluridisciplinaire **HAL**, est destinée au dépôt et à la diffusion de documents scientifiques de niveau recherche, publiés ou non, émanant des établissements d'enseignement et de recherche français ou étrangers, des laboratoires publics ou privés.

Distributed under a Creative Commons CC BY-NC 4.0 - Attribution - Non-commercial use - International License

Version of Record: https://www.sciencedirect.com/science/article/pii/S0584854719304525
Manuscript_225b73aa2505705d7bf35ff5df32c62f

Laser-induced breakdown spectroscopy of uranium in the VUV range

E. Rollin[1], O. Musset[2], D. Cardona[3], J.-B. Sirven[1]

[1] *Den – Service d'Etudes Analytiques et de Réactivité des Surfaces (SEARS), CEA, Université Paris-Saclay, France*
[2] *Université Bourgogne Franche Comté, Laboratoire Interdisciplinaire Carnot Bourgogne, UMR 6303, CNRS, F-21078 Dijon, France*
[3] *CEA, Valduc, F-21120 Is Sur Tille, France*

Abstract

Quantitative analysis of impurities in nuclear materials is necessary in a number of areas, including process control during manufacturing, quality control of products, or for nuclear forensics purposes. Due to the important handling constraints induced by the samples radioactivity and their containment inside airtight enclosures, optical analytical techniques have great advantages over standard ones that require sample preparation, like ICP-based techniques. Therefore, laser-induced breakdown spectroscopy (LIBS) is developed for fast quantitative analysis of impurities in uranium. Actinides are well-known to have a very large number of emission lines in the UV-visible spectral range, hence making the detection of trace or minor elements a real challenge. Therefore, in this study we explored the vacuum ultraviolet range (VUV), i.e. below 200 nm, in order to investigate if this spectral region is more favorable for elemental analysis of uranium by LIBS. As practically no data on VUV spectroscopy of uranium are available, we first analyzed the spectra obtained to assess the spectral density of uranium lines, both in the UV and VUV. Then, the detection limits of two elements, carbon and vanadium, were estimated. It was found that, in spite of a less dense and less intense uranium background in the VUV, this spectral region is not relevant for metal impurities whose spectra are marginally analytically useful in the VUV. Conversely, for non-metals having intense lines in the VUV, the detection limit can be significantly better than in the UV. This was already known for non-nuclear samples. This study extends that conclusion to nuclear materials and has important practical consequences on the implementation of a LIBS analyzer in a nuclear facility.

1. Introduction

Manufacturing and recycling of nuclear materials requires precise knowledge of the composition of those materials. Indeed, during the various steps of production, objects may get contaminated with many different elements. For example, some elements are harmful for the efficiency of the nuclear products, even at ultratrace levels: these are the so-called neutron poisons, such as B, Cd, Sm, Eu, Gd, Dy, Hf and some others, which can cause dramatic neutron losses, hindering the fission reactions [1]. Besides, alkali and alkaline earths affect the efficiency by reducing the density of the product [2]. Moreover, other impurities such as carbon or transition metals (Fe, Ni, V, Cr, Mn…), though not as detrimental as neutron poisons, may also be harmful in the same way as alkali or alkaline earths, and

© 2020 published by Elsevier. This manuscript is made available under the CC BY NC user license
https://creativecommons.org/licenses/by-nc/4.0/

can be common contaminants during the production [3]. Finally, contrary to non-radioactive metals, nuclear materials can produce their own contamination through radioactive decay. These decay products, such as Th, can not only reduce the efficiency of the nuclear fuels, but also raise health concerns because of their sometimes shorter half-life and thus higher radiotoxicity [4].
To monitor all these impurities through the manufacturing processes, various methods are used, but they rely mainly on wet chemistry coupled with lab devices such as ICP-MS and ICP-AES [5,6]. These methods are relatively slow, produce additional wastes and cannot be used directly on the production lines, which sometimes leads to important delays.
In the recent years, Laser-Induced Breakdown Spectroscopy (LIBS) is being developed in different fields of nuclear sciences as a mean to achieve fast analysis of nuclear materials. LIBS is thoroughly described in other papers [7-9] and features some unique perks that make up for its relatively low sensitivity: thanks to its rapidity, compactness, and ability to be used remotely and to detect all elements in one measurement, LIBS can be especially relevant for *in situ* or *online* measurements of nuclear materials. In fact, it has been used by several teams as a mean of achieving quality control, both for the production of nuclear fuel [10,11] and for its recycling [12], for studies on uranium corrosion [13], and is being considered by some authors as a promising method for nuclear safeguards and forensics [5,6,14-16].

Although the typical detection system in LIBS operates in the UV-visible range, LIBS was also developed in the VUV range to analyze metalloids and non-metals, which have intense emission lines below 200 nm, in order to improve their detection limit. Hence, elements such as sulfur, carbon, phosphor, or halogens like chlorine or bromine, were successfully measured in VUV [17-20]. Another motivation of this spectral region is to avoid spectral interferences compared to the UV-visible range [20]. A common case is the analysis of carbon in steel, whose UV emission line at 247.856 nm is interfered by that of iron at 247.857 nm [21,22].

In the case of nuclear materials, this rationale is even more relevant as uranium and plutonium possess a very large number of emission lines in the UV-visible range. The literature reports 92,000 uranium lines between 0.2 and 4.2 µm [23], and 20000 plutonium lines in the visible [24]. Since uranium, like transition metals, displays most of its lines in the UV-visible range and much fewer in VUV, this wavelength range is supposed to be more favorable for analyzing impurities in this matrix. This was demonstrated in the case of GD-OES measurements of carbon, hydrogen, nitrogen and oxygen in nuclear materials [24]. Therefore, the main goal of the present work was to investigate the potential of VUV-LIBS in the detection and quantification of several elements in a uranium matrix.

For that purpose, we focused on two elements having a very different spectroscopy: carbon and vanadium. The quantification of carbon in metal uranium can indeed be quite useful in nuclear forensics: since cast alloys usually have higher carbon concentration than wrought ones, this analysis can be used to determine how the sample has been processed. Overall, carbon and vanadium can be considered representative of two families of possible impurities: first, the light elements, such as C, H, N, O, S, P, with only a few strong spectral lines, with the most intense in VUV or other small wavelengths ranges [18,21,22,25], and second, the transition metals, which present many more emission lines, most of them lying in the UV-visible range. The VUV and UV spectra of uranium obtained were analytically characterized, with a specific focus on the limit of detection attainable for carbon and vanadium.

2. Experimental setup

2.1. Instrumentation

A schematic representation of the experimental setup is displayed in Figure 1. The laser is a Q-Switched Nd:YAG (Quantel Brio) operating at 266 nm (fourth harmonic), delivering pulses of 5 ns and up to 10 mJ at the exit of the laser (5 mJ on the sample surface), at a repetition rate of 20 Hz. A mechanical shutter, an energy attenuator consisting of a half-wave plate and a polarizer, as well as a beam sampling system for energy measurement, are used to control the number and energy of laser pulses on the sample. The laser beam is guided through a beam expander before being focused at normal incidence onto the sample surface by a 250 mm focal length plano-convex lens. This results in a 50 µm diameter spot, estimated by measuring the diameter of an ablation crater in aluminum, leading to an irradiance up to 50 GW/cm² at the sample surface. 50 laser shots were accumulated on each sample location, then the sample was moved so that there was no overlap between successive craters. Each recorded spectrum was the result of 1000 laser shots in total, i.e. accumulated over 20 craters.

The samples are fixed horizontally in a custom-made container (CLM Industrie company) designed specifically for the use of uranium. This container is placed on a XYZ translation platform. The laser enters the container through a fused-silica window and the plasma light propagates to the collection mirror through a 10-mm thick MgF_2 window in order to maximize VUV transmission. The mirror is a spherical concave mirror (eSource Optics) with a 150 mm focal length and coated with Al-MgF_2 with the specific purpose of enhancing the reflectivity of the VUV spectral range. The angle between the vertical axis (direction of the laser beam) and the collection axis is 34°. The container is pumped at a 10^{-4} to 10^{-5} mbar vacuum before its transfer to the vacuum chamber.

The collection mirror focuses the plasma light, through another 10-mm thick MgF_2 window, onto the entrance slit of a 1 m focal length Czerny-Turner spectrometer (Horiba VHR 1000) designed for VUV measurements and equipped with a 3600 lines/mm holographic grating. The distance between the collection mirror and the entrance slit is 600 mm. The slit height is 1 cm and its width is set to 100 µm. The spectrometer is coupled to a CCD camera (Princeton Instruments PIXIS-XO 400B, 1340x400 pixels, 20x20 µm per pixel). The pixels were vertically binned so that the obtained spectra are 1340 pixels wide. The measured linear dispersion and the spectral bandwidth vary respectively from 5 pm/pixel and 7 nm around 150 nm to 2.5 pm/pixel and 3.5 nm around 450 nm. The CCD exposition time was 5 ms, so that spectra were integrated over the whole plasma lifetime.

The sample container, its translation platform, the focusing lens and the collection mirror are all placed in a vacuum chamber with an inside volume of approximately 0.14 m^3. Both the vacuum chamber and the spectrometer are kept at a 10^{-4} to 10^{-5} mbar vacuum in order to enable the transmission of VUV-radiations during all the LIBS experiments. This is achieved with two sets of two pumps: a primary pump (Pfeiffer Vacuum ACP 28) and a turbomolecular pump (Pfeiffer Vacuum HiPace® 80). The sample container is pumped beforehand, separately, using the set of pumps of the vacuum chamber.

Due to the lack of available data on uranium atomic spectroscopy in the VUV range, we also experimentally explored the spectra obtained by ICP-OES (Ametek SpectroBlue). The analyzed solution was a 1000 ppm uranium solution in 2% HNO_3. A standard cross-flow nebulizer with a Scott spray chamber was used. The ICP RF was used with a power of 1450 W, with a plasma gas flow rate of 12 L/min, an auxiliary gas flow rate of 1 L/min, and a nebulizer gas flow rate of 0.71 L/min. The system was equipped with a Paschen-Runge polychromator with 15 CCD detectors covering a spectral range between 165 and 770 nm with a linear dispersion of 0.3 pm/pixel between 160 and 280 nm, 0.6 pm/pixel between 280 and 470 nm. The system collects plasma signal radially.

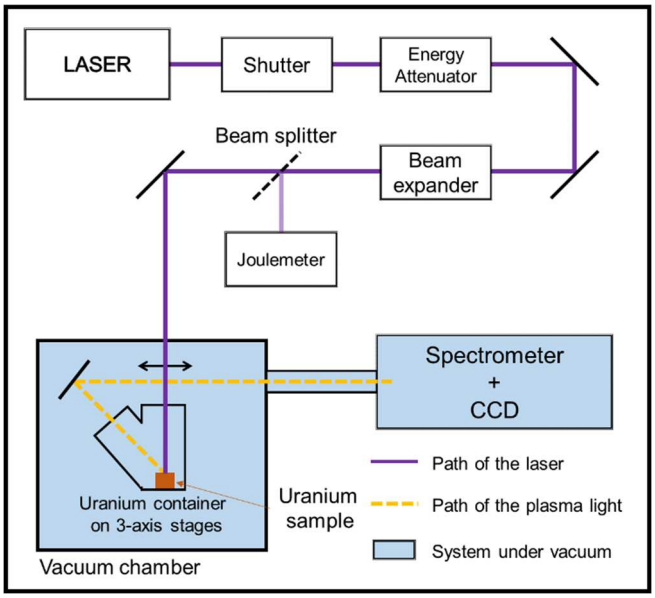

Figure 1 : Experimental setup.

2.2. Samples

The studied samples are small metallic slabs of depleted uranium, roughly shaped as squares of 1 cm x 1 cm weighing approximately 1 g each. They are standard reference samples (CETAMA OPERA 103) containing a certified concentration of carbon as impurity (226 ± 11 ppm) and 0.2 % vanadium as alloying element. Samples were stored in air and their surface was oxidized. However, as 50 laser shots were fired at each sample location, the oxidation layer was ablated by the first shots and we assumed that its influence on the LIBS signal could be neglected.

3. Results and discussion

3.1. Study of uranium spectra in the VUV range

Figure 2 shows the spectra of uranium obtained in two spectral windows in the UV and VUV ranges, around 159 nm and 309 nm, respectively. Several observations can be made. First, the density of detectable lines is very different. The UV spectrum is highly structured. This structure is not noise, it is due to the overlap of many uranium lines. This assumption is supported by the publication of Blaise et al. who identified 92,000 emission lines of U I and U II between 200 nm and 4.2 µm [23]. On the contrary, the VUV spectrum is much smoother with a few lines emerging from the background. This observation is consistent with that reported in previous works on GD-OES analysis of impurities in uranium [24], although the sampling and excitation mechanisms are different in LIBS. This suggests that the VUV region is less prone to spectral interferences by uranium lines, and therefore could be more favorable for analytical purposes in this regard.

However, as observed on Figure 2, the apparent signal-to-background ratio of uranium spectra is rather low both in the VUV and UV ranges. The spectral background is attributed to the continuous background due to Bremsstrahlung and radiative recombination, and to the overlap of unresolved uranium emission lines. To further investigate both contributions, Figure 2 compares uranium spectra to spectra of an aluminum alloy obtained in the same conditions. Aluminum has very few emission lines, and the resolving power of the spectrometer is high enough to allow the conclusion that no significant spectral interferences should be present. Hence, the spectral background of aluminum spectra is attributed solely to the continuous background, which is intense immediately

after the laser shot but decreases very rapidly [26,27]. Yet, it is not zero since spectra are integrated by the CCD detector over the whole plasma persistence.

As seen in both spectral regions, the uranium background is 2-3 times higher than that of aluminum. Although the continuum level is a complex function of the plasma temperature and density [7], which are supposed to be different between aluminum and uranium, the comparison of spectra suggests that indeed, the contribution of unresolved lines to the spectral background of uranium is important, including in the VUV range.

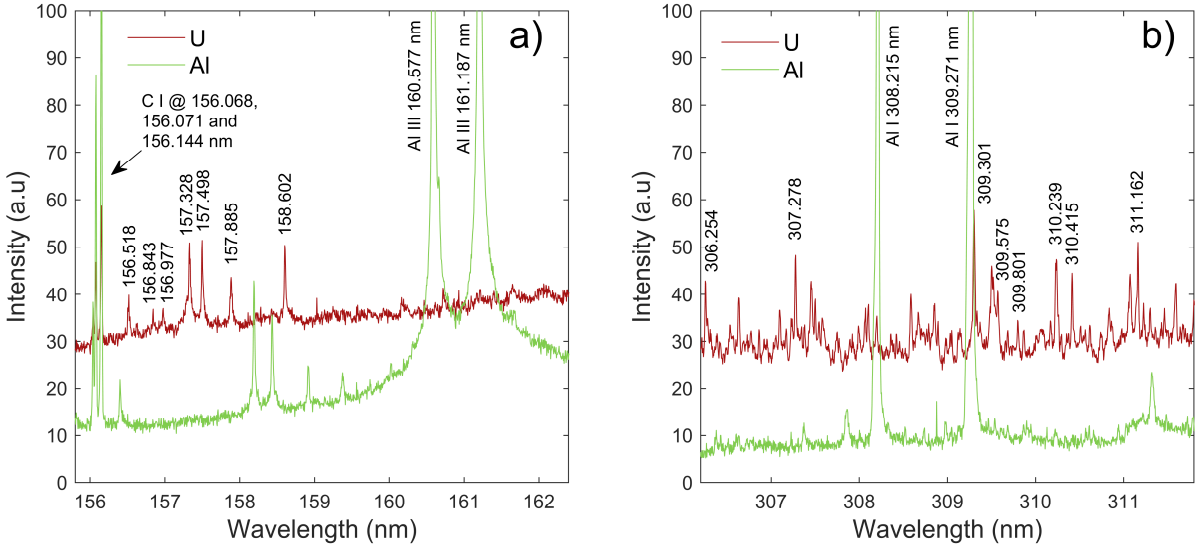

Figure 2: Comparison of LIBS spectra of uranium and aluminum alloys in the VUV (a) and UV-visible (b) ranges. Labels show the wavelength of the most intense observed lines. In the UV-visible spectrum, wavelengths were retrieved from the NIST database [28].

Observation of the ICP-OES spectrum of the uranium solution, shown in Figure 3, provides further insight into the contribution of unresolved lines in the background observed in LIBS. From Boltzmann plots based on the U II lines used by Akpovo et al. [29], the ICP electron temperature was found to be approximately 10% lower than that of the LIBS plasma in the vacuum. Contrary to LIBS measurements, however, no neutral uranium lines were detected in ICP-OES spectra. From the Saha equation, this means that the electron number density is significantly lower in ICP than in LIBS, leading to a much less pronounced line broadening by the Stark effect. Therefore, thinner emission lines and a negligible continuous background are expected in ICP compared to LIBS. As shown in Figure 3, in the VUV range the full width at half maximum of lines measured by ICP-OES is 7 pm, approximately 3 times lower than in LIBS (20 pm with the spectrometer used in this study). In spite of that, we can observe that the ICP-OES background is not equal to zero, and that the number of uranium emission lines in VUV is higher than what one may have expected. Lines with a signal-to-background ratio higher than 5 are still common and smaller lines cover the whole spectrum.

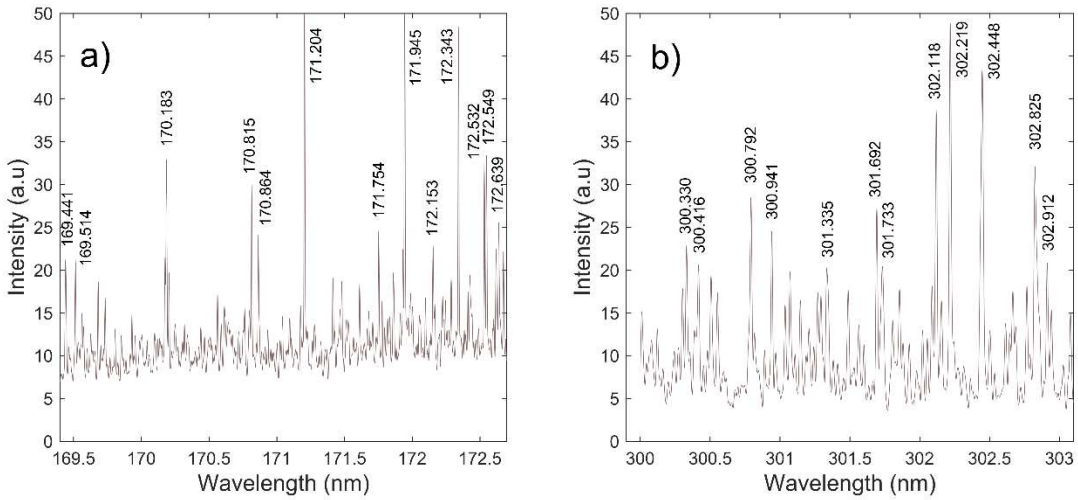

Figure 3 : ICP-OES spectra of a 1g/L uranium solution in the VUV (a) and UV-visible (b) ranges. The spectrum of the solvent has been subtracted. Labels show the wavelength of the most intense observed lines.

One can then conclude that even though uranium displays fewer intense lines in the VUV range, which could facilitate the avoidance of spectral interferences, it has still enough weak emission lines that cause a relatively high spectral background. In LIBS, those lines result in an apparently continuous background that adds to the usual background due to electron collisions and recombination, which is especially prominent in early stages in the plasma lifetime. This is all the more problematic in LIBS as the lines are broadened by the Stark effect, which is less pronounced in ICP- or GD-OES for instance. Finally, the VUV range is not necessarily more favorable than the UV one from this point of view, and its interest for the detection and quantitation of impurities by LIBS is not obvious. This will be addressed in more details in the next section in the case of carbon and vanadium.

3.2. Detection of impurities in uranium in the UV and VUV ranges

The spectra of carbon in uranium are shown on Figure 4 around two emission lines, one in UV-visible at 247.856 nm commonly used for carbon quantification, and the other one in the VUV range at 165.701 nm. This line was chosen instead of the more widely used one at 193.091 nm, for its proximity to vanadium lines of interest around the same wavelength. The two selected carbon lines and their spectroscopic parameters are detailed in Table 1. Note that between 165.5 and 166 nm, other carbon lines are visible on both sides of the 165.701 nm one, whereas the UV one is surrounded by uranium lines. The VUV range clearly seems more favorable, since the line intensity is higher than in UV, and the possible interferences with uranium lines are much more limited.

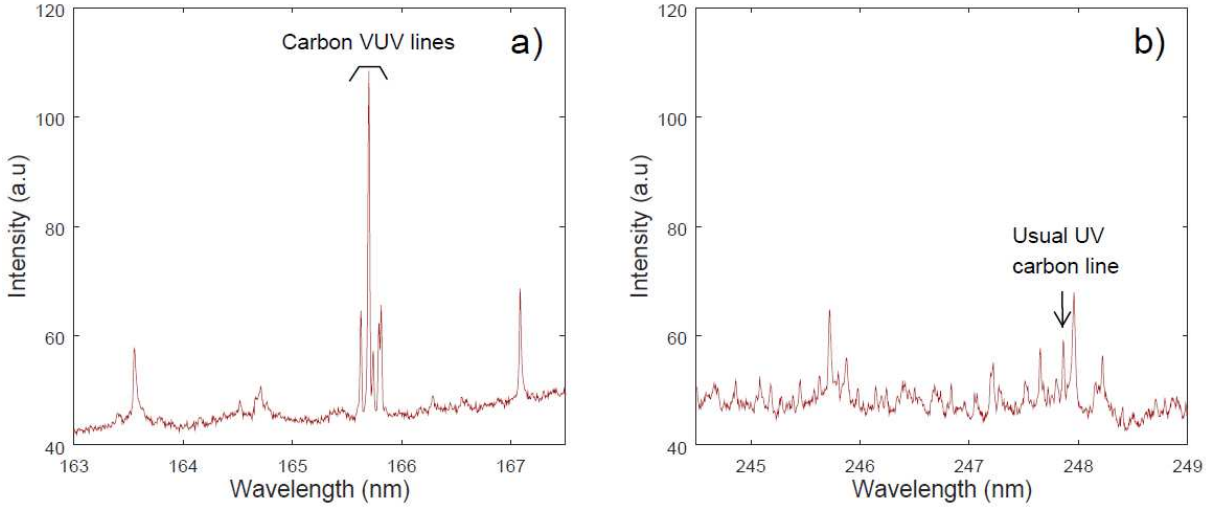

Figure 4: Emission lines of 226 ppm carbon in uranium in the VUV (a) and UV-visible (b) ranges. Each spectrum is an average of 20 replica of 250 laser shots.

To go further, we determined the limit of detection (LOD) of carbon in our experimental conditions. Since we had only one sample, we calculated it from the signal-to-noise ratio (SNR) of carbon lines using the following expression:

$$LOD = \frac{3\,c}{SNR} = \frac{3\,\sigma_B}{I}\,c \sim \frac{3\,\sigma_B}{s} \qquad (1)$$

where σ_B is the standard deviation of the spectral background in the vicinity of the emission line measured from 20 replica, I is the line intensity as measured in the experiment, and c is the carbon concentration in the sample. It is worth noting that in this expression, the ratio I/c is taken as an estimate of the slope of the calibration curve s, assuming it is linear at the carbon concentration level. The LOD determination will be more precise using a proper calibration, which would require a set of calibration samples.

We obtained a LOD of 25 ppm for the VUV carbon line, and 150 ppm for the UV one. This shows that the use of VUV greatly improves the detection of carbon in a uranium matrix, by a factor of 6 in the present case. This is consistent with the existing literature on LIBS analysis of carbon in the VUV range for other matrices (particularly steel) [22,30], and also with the work of Lavoine et al. on GD-OES analysis of this element in nuclear materials [24]. It confirms that both for spectroscopic reasons and due to less pronounced spectral interferences, the VUV range is relevant for quantitative analysis of carbon in uranium by LIBS.

Table 1 spectroscopic data of two carbon (C I) emission lines observed in uranium

Wavelength (nm)	E_i (eV)	E_j (eV)	g_j	A_{ji} (10^8 s^{-1})
165.701	0.01	7.49	5	2.61
247.856	2.68	7.68	3	0.28

Since the uranium samples include approximately 0.2 % of vanadium, we also evaluated the detection limit of this element in uranium. Spectra obtained in the UV and VUV spectral ranges are shown on Figure 5, as well as spectra of pure vanadium obtained in analogous conditions, as a mean of comparison in order to clearly identify, among the numerous uranium lines, the emission lines of

vanadium. Those lines are labeled on Figure 5 from the NIST database [28], and the most favorable ones are listed in Table 2.

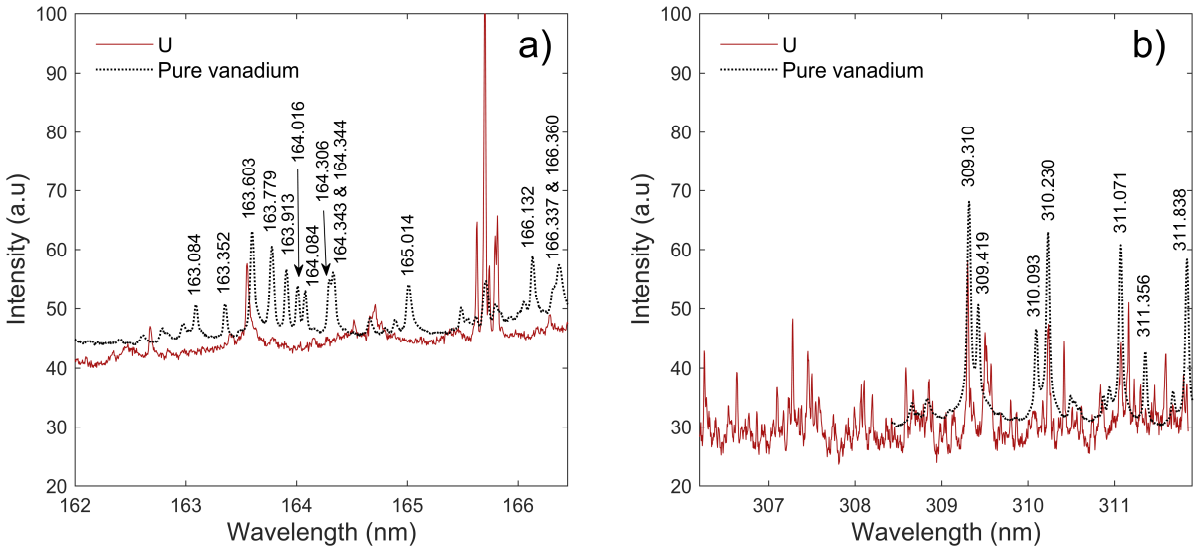

Figure 5 : Emission spectrum of uranium with 0.2 % vanadium compared to pure vanadium in VUV (a) and UV-visible (b) ranges. Labels show the wavelength of the most intense observed lines of vanadium.

Unfortunately, no VUV line of vanadium has been detected. Only lines in the UV-visible range have been observed, especially around 310 nm, where the most intense lines of the V II emission spectrum can usually be found. Many uranium lines are present in this spectral range. The observation of LIBS and ICP-OES spectra showed that the vanadium lines at 309.310 and 310.230 nm interfered significantly with a uranium one, measured respectively at 309.301 and 310.243 nm. Whereas the 311.071 nm line was found less affected by the presence of uranium, the two closest detectable lines being at 311.053 and 311.084 nm. Thus, in order to evaluate the LOD of vanadium, the 311.071 nm line was chosen.

Table 2: Spectroscopic data of UV and VUV emission lines of vanadium (V II)

Wavelength (nm)	E_i (eV)	E_j (eV)	g_j	A_{ji} (10^8 s^{-1})
163.603	0.39	7.97	11	2.45
309.310	0.39	4.40	13	2.00
310.230	0.37	4.36	11	1.78
311.071	0.35	4.33	9	1.58

The LOD of vanadium has been estimated using the same approach as for carbon, from the measured intensity of the 311.071 nm emission line. We found an LOD of about 1000 ppm. This value is probably overestimated, for the spectral background under the vanadium line is difficult, if not impossible, to measure correctly due to the presumed density of uranium lines (see section 3.1). This leads to an overestimation of the background level and of its fluctuation σ_B, but also to an underestimation of the net intensity of the line, whose wings are hidden by the background.

However, even assuming a bias in the intensity measurement due to spectral interferences, the detection limit of vanadium is surprisingly high (i.e., worse) compared to that of carbon in the UV range. This can be attributed to a surface enrichment in carbon. Indeed, we observed a significant decrease of the carbon LIBS signal with the number of laser shots at a given sample location. Therefore, the average carbon concentration in the sample thickness probed by the LIBS analysis is larger than the certified concentration, of 226 ppm, leading to an optimistic determination of the

carbon LOD. In the framework of this study, it was not possible to test this assumption. A GD-OES analysis, for instance, would enable to check it.

The fact remains that vanadium was not detected in the VUV range in our experimental conditions. This is coherent with the observed intensities of its UV-visible lines, which were relatively low as they led to a high LOD: as shown in Table 2, the VUV line (163.600 nm, supposedly the most intense of the observed spectral range) has an excitation energy much higher than the UV lines, making it harder to detect. This, added to the fact that a lower collection efficiency is to be expected in VUV than in UV, probably explains why the vanadium did not show up in the VUV region while it did in UV-visible range.

As a summary, the observations of the VUV region enabled us to enhance the carbon detection compared to the UV-visible range, whereas an opposite result has been found for the detection of vanadium.

4. Conclusion

In this paper we studied the feasibility of quantitative analysis of carbon and vanadium in metal uranium by LIBS in the vacuum, in the VUV and UV spectral ranges, using a time-integrated detection system. One major motivation of this work was to investigate the analytical interest of the VUV range for uranium analysis, particularly in view of the spectral interferences with such a line-rich matrix.
We found that, although in the VUV range the density of detectable uranium lines is lower than in the UV range, the spectral background remains relatively high. This background can be partially attributed to unresolved, weaker uranium lines.
The detection limits of carbon and vanadium were evaluated. For carbon, an LOD of 25 ppm was obtained in the VUV range using the 165.701 nm line and 150 ppm in the UV range with the 247.856 nm line, clearly demonstrating the interest of VUV detection in such a complex matrix as uranium.
For vanadium, the detection limit was estimated at 1000 ppm using the 311.071 nm line. Vanadium was not detected in the VUV range.
Our results on carbon are consistent with the existing literature in LIBS analysis of carbon in more conventional materials, and with previous works on GD-OES measurements of carbon in nuclear materials [24]. The results obtained on vanadium are more surprising and deserve further investigation. One way of potentially improving the performances in the UV range for this element would be to use an intensified CCD, so as to take advantage of temporal resolution in order to optimize the analytical signal.
We finally note that this study has important practical consequences on the implementation of a LIBS analyzer in nuclear environment. Although VUV-LIBS has shown some advantages for the detection of carbon and probably other light elements, it has not been suitable for the detection of vanadium. Since operation and maintenance of a system under vacuum, coupled to airtight enclosures used for containment of nuclear materials, are difficult, VUV-LIBS in nuclear conditions may only be justified for some analytes of interest. In a more general case, UV-visible LIBS can be chosen as it enables a simpler experimental setup.

5. Acknowledgements

The authors would like to thank Adeline Masset, Gabriel Lambrot and Pascal Fichet for providing the ICP-OES spectra.

6. References

[1] R. K. Malhotra and K. Satyanarayana, “Estimation of trace impurities in reactor-grade uranium using ICP-AES,” Talanta, vol. 50, no. 3, pp. 601–608, Oct. 1999.

[2] P. Verma and K. L. Ramakumar, “Determination of alkali and alkaline earth elements along with nitrogen in uranium based nuclear fuel materials by ion chromatography (IC),” Anal. Chim. Acta, vol. 601, no. 1, pp. 125–129, Oct. 2007.

[3] A. L. de Souza, M. E. B. Cotrim, and M. A. F. Pires, “An overview of spectrometric techniques and sample preparation for the determination of impurities in uranium nuclear fuel grade,” Microchem. J., vol. 106, pp. 194–201, Jan. 2013.

[4] D. D. Reilly, M. T. Athon, J. F. Corbey, I. I. Leavy, K. M. McCoy, and J. M. Schwantes, “Trace element migration during UF4 bomb reduction: Implications to metal fuel production, worker health and safety, and nuclear forensics,” J. Nucl. Mater., vol. 510, pp. 156–162, Nov. 2018.

[5] K. R. Campbell et al., “Laser-induced breakdown spectroscopy of light water reactor simulated used nuclear fuel: Main oxide phase,” Spectrochim. Acta Part B At. Spectrosc., vol. 133, pp. 26–33, Jul. 2017.

[6] K. Campbell, “A promising tool for Nuclear Safeguards : Laser-Induced Breakdown Spectroscopy,” Actin. Res. Q., 2018.

[7] D. W. Hahn and N. Omenetto, “Laser-Induced Breakdown Spectroscopy (LIBS), Part I: Review of Basic Diagnostics and Plasma–Particle Interactions: Still-Challenging Issues Within the Analytical Plasma Community,” Appl. Spectrosc., vol. 64, no. 12, pp. 335–366, Dec. 2010.

[8] D. W. Hahn and N. Omenetto, “Laser-Induced Breakdown Spectroscopy (LIBS), Part II: Review of Instrumental and Methodological Approaches to Material Analysis and Applications to Different Fields,” Appl. Spectrosc., vol. 66, no. 4, pp. 347–419, Apr. 2012.

[9] C. Aragón and J. A. Aguilera, “Characterization of laser induced plasmas by optical emission spectroscopy: A review of experiments and methods,” Spectrochim. Acta Part B At. Spectrosc., vol. 63, no. 9, pp. 893–916, Sep. 2008.

[10] M. Singh, A. Sarkar, X. Mao, and R. E. Russo, “Direct compositional quantification of (U-Th)O2 - MOX nuclear fuel using ns-UV-LIBS and chemometric regression models,” J. Nucl. Mater., vol. 484, pp. 135–140, Feb. 2017.

[11] P. Fichet, P. Mauchien, and C. Moulin, “Determination of Impurities in Uranium and Plutonium Dioxides by Laser-Induced Breakdown Spectroscopy,” Appl. Spectrosc., vol. 53, no. 9, pp. 1111–1117, Sep. 1999.

[12] X. Wang et al., “Mapping of rare earth elements in nuclear waste glass–ceramic using micro laser-induced breakdown spectroscopy,” Spectrochim. Acta Part B At. Spectrosc., vol. 87, pp. 139–146, Sep. 2013.

[13] E. Garlea et al., “Novel Use of a Hand-Held Laser Induced Breakdown Spectroscopy Instrument to Monitor Hydride Corrosion and Microstructure Effects in Uranium,” Spectrochimica Acta Part B At. Spectrosc., vol. 159, p. 105651, Sept. 2019.

[14] J. E. Barefield et al., “Analysis of geological materials containing uranium using laser-induced breakdown spectroscopy,” Spectrochim. Acta Part B At. Spectrosc., vol. 120, pp. 1–8, Jun. 2016.

[15] J.-B. Sirven, A. Pailloux, Y. M’Baye, N. Coulon, T. Alpettaz, and S. Gossé, “Towards the determination of the geographical origin of yellow cake samples by laser-induced breakdown spectroscopy and chemometrics,” J. Anal. At. Spectrom., vol. 24, no. 4, pp. 451–459, 2009.

[16] M. Martin et al., “Micro-Laser-Induced Breakdown Spectroscopy: A Novel Approach Used in the Detection of Six Rare Earths and One Transition Metal,” Minerals, vol. 9(2), p. 103, Feb. 2019.

[17] I. Radivojevic, C. Haisch, R. Niessner, S. Florek, H. Becker-Ross, and U. Panne, “Microanalysis by Laser-Induced Plasma Spectroscopy in the Vacuum Ultraviolet,” Anal. Chem., vol. 76, no. 6, pp. 1648–1656, Mar. 2004.

[18] J. Jasik, J. Heitz, J. D. Pedarnig, and P. Veis, “Vacuum ultraviolet laser-induced breakdown spectroscopy analysis of polymers,” Spectrochim. Acta Part B At. Spectrosc., vol. 64, no. 10, pp. 1128–1134, Oct. 2009.
[19] I. Radivojevic, R. Niessner, C. Haisch, S. Florek, H. Becker-Ross, and U. Panne, “Detection of bromine in thermoplasts from consumer electronics by laser-induced plasma spectroscopy,” Spectrochim. Acta Part B At. Spectrosc., vol. 59, no. 3, pp. 335–343, Mar. 2004.
[20] L. Radziemski, D. A. Cremers, K. Benelli, C. Khoo, and R. D. Harris, “Use of the vacuum ultraviolet spectral region for laser-induced breakdown spectroscopy-based Martian geology and exploration,” Spectrochim. Acta Part B At. Spectrosc., vol. 60, no. 2, pp. 237–248, Feb. 2005.
[21] M. A. Khater, J. T. Costello, and E. T. Kennedy, “Optimization of the Emission Characteristics of Laser-Produced Steel Plasmas in the Vacuum Ultraviolet: Significant Improvements in Carbon Detection Limits,” Appl. Spectrosc., vol. 56, no. 8, pp. 970–983, Aug. 2002.
[22] M. A. Khater, “Laser-induced breakdown spectroscopy for light elements detection in steel: State of the art,” Spectrochim. Acta Part B At. Spectrosc., vol. 81, pp. 1–10, Mar. 2013.
[23] J. Blaise and L. J. Radziemski, “Energy levels of neutral atomic uranium (UI),” JOSA, vol. 66, no. 7, pp. 644–659, 1976.
[24] V. Lavoine, H. Chollet, J.-C. Hubinois, S. Bourgeois, and B. Domenichini, “Optical interfaces in GD-OES system for vacuum far ultraviolet detection,” J. Anal. At. Spectrom., vol. 18, no. 6, pp. 572–575, 2003.
[25] P. Veis, A. Marín-Roldán, and J. Krištof, “Simultaneous vacuum UV and broadband UV–NIR plasma spectroscopy to improve the LIBS analysis of light elements,” Plasma Sources Sci. Technol., vol. 27, no. 9, p. 95001, 2018.
[26] K. H. Kurniawan, M. O. Tjia, and K. Kagawa, “Review of Laser-Induced Plasma, Its Mechanism, and Application to Quantitative Analysis of Hydrogen and Deuterium,” Appl. Spectrosc. Rev., vol. 49, no. 5, pp. 323–434, Jul. 2014.
[27] S. S. Harilal, P. K. Diwakar, N. L. LaHaye, and M. C. Phillips, “Spatio-temporal evolution of uranium emission in laser-produced plasmas,” Spectrochim. Acta Part B At. Spectrosc., vol. 111, pp. 1–7, Sep. 2015.
[28] “NIST: Atomic Spectra Database Lines Form.” [Online]. Available: http://physics.nist.gov/PhysRefData/ASD/lines_form.html. [Accessed: 16-Mar-2017].
[29] C. A. Akpovo, A. Ford, and L. Johnson, “Optimized LWIR enhancement of nanosecond and femtosecond LIBS uranium emission,” Appl. Phys. B, vol. 122, no. 5, p. 154, May 2016.
[30] V. Sturm, L. Peter, and R. Noll, “Steel Analysis with Laser-Induced Breakdown Spectrometry in the Vacuum Ultraviolet,” Appl. Spectrosc., vol. 54, no. 9, pp. 1275–1278, Sep. 2000.

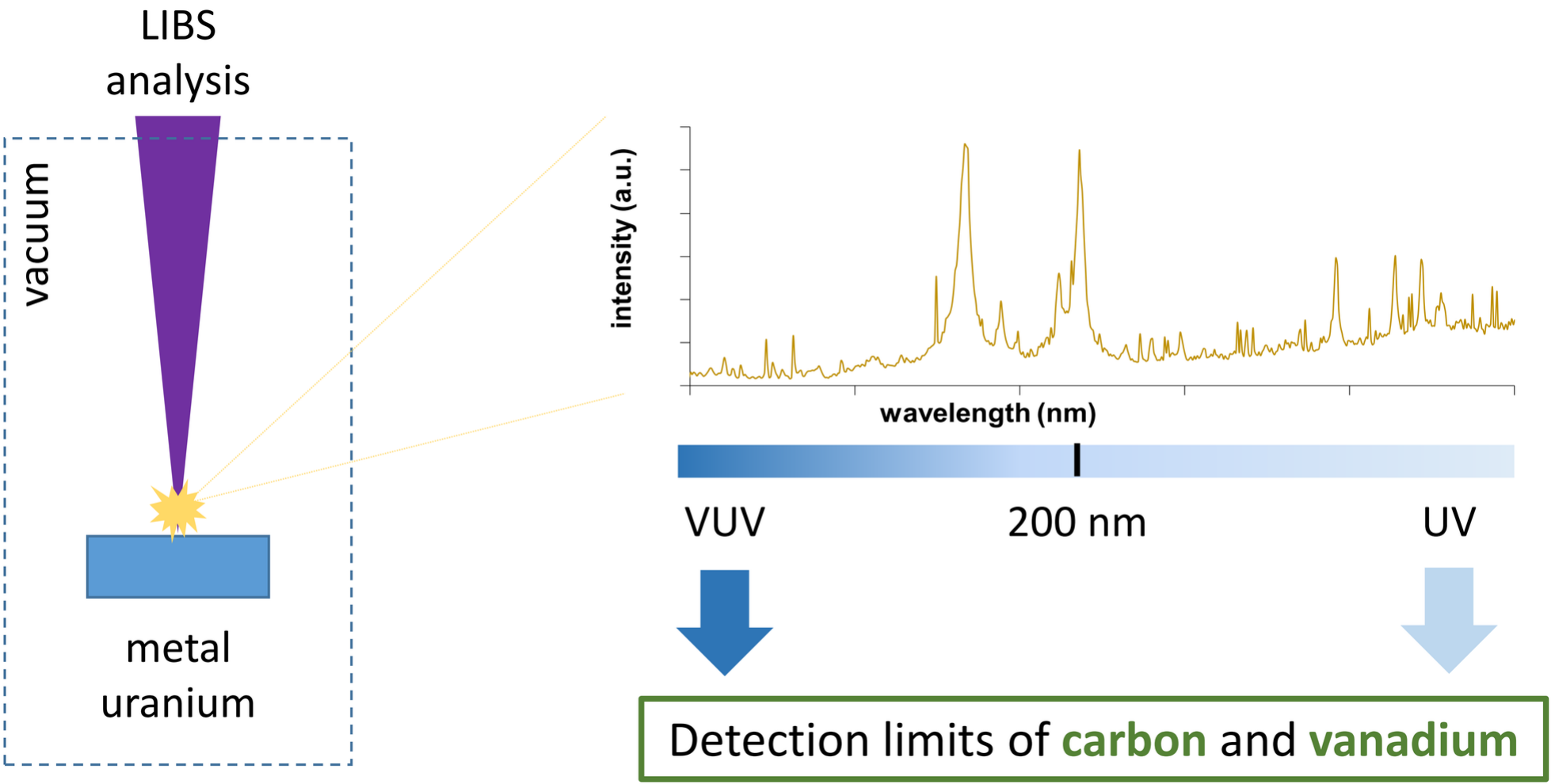
LIBS
analysis
vacuum
metal
uranium
intensity (a.u.)
wavelength (nm)
VUV
200 nm
UV
Detection limits of carbon and vanadium